Scripta Materialia 136 (2017) 106–110

Contents lists available at ScienceDirect

Scripta Materialia

journal homepage: www.elsevier.com/locate/scriptamat

Regular article

Superelastic fatigue of columnar-grained Cu-Al-Mn shape memory alloy under cyclic tension at high strain

Ji-Li Liu [a,b], Hai-You Huang [b,*], Jian-Xin Xie [b], Shuang Xu [a], Fang Li [a]

[a] Hubei Key Laboratory of Theory and Application of Advanced Materials Mechanics, School of Science, Wuhan University of Technology, Wuhan 430070, China
[b] Beijing Laboratory of Metallic Materials and Processing for Modern Transportation, University of Science and Technology Beijing, Beijing 100083, China

ARTICLE INFO

Article history:
Received 27 February 2017
Received in revised form 28 March 2017
Accepted 12 April 2017
Available online xxxx

Keywords:
Shape memory alloy
Cu-Al-Mn
Columnar grain
Superelasticity
Functional fatigue

ABSTRACT

Columnar-grained Cu-Al-Mn shape memory alloy (SMA) exhibits excellent superelastic fatigue properties at high strain amplitude, and its functional fatigue life reaches above 10^3 cycles at tensile strain of 4%–10%. As the increase of loading-unloading cycle number, the transformation stress and superelastic recovery rate decrease. The decay coefficient of recovery rate is about 1.4. Fatigue cycles for Cu-Al-Mn SMAs can be divided into four stages according to the significant changes of superelasticity: plateaus stage, rapid attenuation earlier stage, rapid attenuation later stage, functional incapacitation stage. The columnar-grained Cu-Al-Mn SMA shows larger range of stable superelasticity than other polycrystalline counterparts.

© 2017 Acta Materialia Inc. Published by Elsevier Ltd. All rights reserved.

Recently, shape memory alloys (SMAs) have attracted considerable attention as damping energy absorption and solid-state refrigeration materials due to their unique reversible martensite transformation and entropy change that absorb mechanical energy and thermal energy [1-7]. In these applications, SMAs are required to have high superelastic strain (e.g., in the case of seismic protection and elastocaloric refrigeration) and reused many times under large cyclic strain with high strain recovery rate. So fatigue is one of the most important properties in SMAs that requires thorough scrutiny. According to the definition by Eggeler et al. [8], fatigue in SMAs is classified into functional fatigue and structural fatigue, which should be considered simultaneously. Structural fatigue is the fracture caused by cyclic loading. In contrast, functional fatigue does not result in fracture. A type of functional fatigue in SMAs is the gradual loss of superelasticity under mechanical cycling.

The single crystalline (SC) Cu-based SMAs, such as SC Cu-Al-Ni [9,10], Cu-Zn-Al [10,11], Cu-Al-Be [12] and Cu-Al-Mn [13] have good fatigue resistance and their fatigue lives can reach hundreds of cycles under a high cyclic strain (>4%). Due to high manufacturing cost and size limitations in producing single crystals, the cheap polycrystalline Cu-based SMAs have been studied intensely. However, the maximum recovery strain of ordinary polycrystalline Cu-based SMAs is about 2–5%, which is less than half of that of SC Cu-based SMAs and polycrystalline Ni-Ti SMAs [14,15], let alone a high fatigue life [16,17]. Based on the idea of microstructure design [18,19], some special polycrystalline Cu-based SMAs, such as bamboo-like-grained (BLG) and columnar-grained (CG) Cu-based SMAs have been designed to obtain huge grain size, high grain-boundary coordination ability and strong texture, which really contribute to achieve high superelastic strain [20–23]. In our previous research [22,24], CG Cu-Al-Mn SMAs showed a high superelastic strain >7% and nearly 100% recovery rate at the first loading-unloading cycle, which reach to the level of SC Cu-based or Ni-Ti SMAs and make it possible to realize the applications of Cu-based SMAs into damping and refrigeration devices.

CG Cu-Al-Mn SMAs have straight grain boundaries morphology, high proportion of low-energy grain boundaries and strong ⟨001⟩-oriented texture along the solidification direction (SD) [18,22]. Transgranular fracture occurs in CG Cu-Al-Mn SMAs during the stretching process, which is similar to single crystal. The increase of ductility and superelasticity in CG Cu-Al-Mn SMAs may indicate that their fatigue properties are different from those in ordinary polycrystalline alloys. In addition, researches on the superelastic fatigue properties of Cu-based SMAs under low strain (<4%) have been reported in many literatures [9,25,26], and most of them mainly focus on SC alloys. The fatigue mechanism of single crystal without grain boundary may not be applicable to polycrystalline microstructure. And in practice, the application requirement for high strain recovery must be taken into account. In this paper, the functional fatigue of Cu-Al-Mn SMA in large strain (>4%) during strain-controlled superelastic cyclic tension is mainly studied.

CG Cu-Al-Mn SMA ingots with the composition of Cu-17.8 at.%Al–11.4 at.%Mn were prepared by unidirectional solidification technique [9,25,26]. Martensite starting temperature and finishing temperature, as well as austenite starting temperature and finishing temperature of

* Corresponding author.
E-mail address: huanghy@mater.ustb.edu.cn (H.-Y. Huang).

http://dx.doi.org/10.1016/j.scriptamat.2017.04.017
1359-6462/© 2017 Acta Materialia Inc. Published by Elsevier Ltd. All rights reserved.

the alloy are −47.2 °C, −64.6 °C, −54.1 °C and −36.6 °C, respectively, which were determined by differential scanning calorimetry. The microstructure characteristics of the CG Cu-Al-Mn sample, such as straight grain boundaries and strong ⟨001⟩-oriented texture along the SD were confirmed by optical photo of the longitudinal section as shown in Fig. 1a and electron backscattered diffraction [24,27]. Fig. 1b shows the calculated tensile transformation strain of the Cu-Al-Mn alloy corresponding to the crystallographic orientation illustrated in a contour chart [22, 28], and the ⟨001⟩-oriented sample has a high transformation strain of ~10%. The cyclic tensile samples with the gage size of ⌀5 × 15 mm^3 and long direction along SD, as shown in Fig. 1c, were cut from the middle of the ingots, where has good columnar-grained microstructure as described in the previous papers [24,27]. Cyclic tensile tests were carried out with an electro-hydraulic servo fatigue testing machine. The cyclic tensile samples were loaded to a target strain, followed by unloading to zero stress in each cycle at room temperature. The number of loading-unloading cycles was above 1000 for all tests. The target strain amplitudes were set at 4%, 6%, 8% and 10%, and were monitored using a 10 mm extensometer. The strain loading and unloading rate were 5×10^{-3} s^{-1}.

The schematic superelastic stress-strain curve of a single cycle stretched along the SD is also shown in Fig. 1c. Based on this curve, some superelastic parameters can be obtained. As seen in Fig. 1c, N is the cycle number, σ_{Ms}^N is the martensite transformation critical stress. ε_t^N is the total loading strain applied to the samples, ε_r^N is the accumulative residual strain after unloading, ε_e^N is the genuine elastic strain, and the superelastic strain ε_{SE}^N of the N-th cycle can be calculated by $\varepsilon_{SE}^N = \varepsilon_t^N - \varepsilon_r^N - \varepsilon_e^N$. $d\sigma_{SE}/d\varepsilon$ is the slope of martensite transformation platform.

The samples stretched to the strain amplitudes of 4%, 6%, 8% and 10% are denoted as CG-4%, CG-6%, CG-8% and CG-10%, respectively. Their stress-strain curves after cyclic loading-unloading are shown in Fig. 2. The plots have been presented at the representative cycles of 1, 2, 5, 10, 20, 50, 100, 200, 400, 700, 1000, 1600 and 2400. No sample fractured up to 1000 cycles. For four strain amplitudes, all samples showed similar fatigue behaviors. Flag-shaped hysteretic loops with excellent superelasticity are observed at first cycles, and then the decays of transformation platform slope, recovery strain and transformation stress can be observed. According to the cyclic stress-strain curves, the variation of property parameters with increasing cycle number can be obtained.

Fig. 3a shows the variation of $d\sigma_{SE}/d\varepsilon$ with increasing cycle number. The $d\sigma_{SE}/d\varepsilon$ of the CG samples almost stabilizes in the range of 0.7–1.4 GPa at first hundred cycles under all of the four loading strains, which indicates the CG alloy can be reused for 100 cycles at least with a relatively stable and low hardening rate of martensite transformation, even under a very high loading strain (e.g. 10%). Then $d\sigma_{SE}/d\varepsilon$ gradually increase and the deviations between the samples under different loading strains are more obvious.

As seen from Fig. 2, the stress of subsequent transformation stage is lower compared with the previous one. The ratio of σ_{Ms}^N and σ_{Ms}^1 was used to quantitatively reflect the decay of martensitic transformation critical stress. Fig. 3b shows the variation of $\sigma_{Ms}^N/\sigma_{Ms}^1$ with increasing cycle number at various strain amplitudes. It can be seen that σ_{Ms}^N decreases as cycle number increases, which is the same as other SMAs [26,29]. In addition, the decreasing rate rises with the increase of strain amplitude. For example, σ_{Ms}^N of 241–268 MPa ($\sigma_{Ms}^N/\sigma_{Ms}^1 \geq 0.9$) was observed at the first cycle to the 150th cycle for CG-4% sample, but the similar $\sigma_{Ms}^N/\sigma_{Ms}^1$ value (~0.9) can be obtained at the 35th, 20th and 14th cycles for CG-6%, CG-8% and CG-10%, respectively. Then σ_{Ms}^N decreases rapidly down to <100 MPa for more cycles. When σ_{Ms}^N decreased to the half value of the first cycle, i.e., $\sigma_{Ms}^N/\sigma_{Ms}^1 = 0.5$, the cycle numbers are corresponding to 2180, 1303, 341 and 322 for the samples under four strain amplitudes. It is noteworthy that the change of the $\sigma_{Ms}^N/\sigma_{Ms}^1$ in CG-8% and CG-10% samples are close to each other. This is possibly attributed to 8%–10% strain is near to the maximum transformation strain (~10%) of ⟨001⟩-oriented CG Cu-Al-Mn alloy, which make these two samples have similar transformation degree and show similar change of σ_{Ms}^N. It is should be noted that σ_{Ms}^N of CG Cu-Al-Mn alloy has less change during the cyclic tension (<6 MPa between the N and N-1 cycle) than those of ordinary polycrystalline Cu-based SMAs [26,30]. This may be due to the better grain-boundary coordination and weaker blockage effect of the low-energy grain boundaries in CG alloy on phase transformation or dislocations slipping.

Residual strain and recovery strain are two of the most important functional fatigue parameters, which directly represent the quantitative measure of superelasticity during the loading history. The ratio of residual strain ε_r and strain $\varepsilon_t - \varepsilon_e$ (including the superelastic and residual strain) in the N-th cycle is taken as the relative value of the residual strain. So the superelastic recovery rate is expressed as $1 - \varepsilon_r / (\varepsilon_t - \varepsilon_e)$. Fig. 3c and d shows the variation of ε_r and $1 - \varepsilon_r / (\varepsilon_t - \varepsilon_e)$, responsively, with the increase of cycle number. In order to compare the fatigue properties of different microstructure Cu-Al-Mn alloy, the data of SC and BLG Cu-Al-Mn alloys reported in literatures [13,23] with the similar chemical component are also plotted in Fig. 3c and d.

It can be seen from Fig. 3c that as the increase of cycle number, ε_r increases due to the accumulation of un-reversible martensite. For CG-4% sample, up to about 2000 cycles, excellent strain recovery is observed with $\varepsilon_r \leq 1\%$, which is corresponding to about 500, 150 and 80 cycles

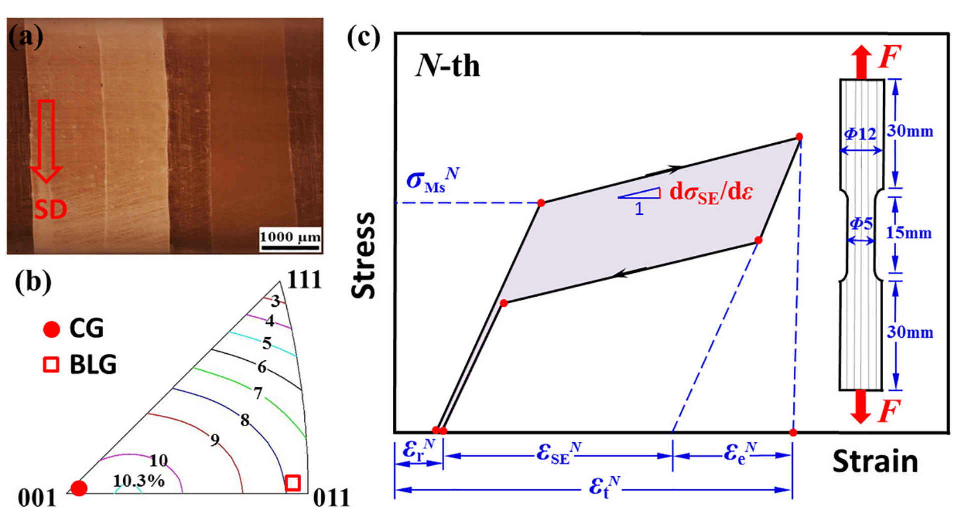

Fig. 1. (a) Longitudinal section microstructure of CG Cu-Al-Mn alloy, (b) contour lines of calculated tensile transformation strain of Cu-Al-Mn alloy with the crystallographic orientation, the grain orientation of CG Cu-Al-Mn alloy in this paper and BLG Cu-Al-Mn alloy in Ref. [23] are marked with symbol ● and □, respectively, (c) sketch diagram of cyclic tensile sample and properties parameters based on superelastic cyclic stress-strain curve.

Download English Version:

https://daneshyari.com/en/article/5443640

Download Persian Version:

https://daneshyari.com/article/5443640

Daneshyari.com